Polyurethane Cationomers with Pendant Trimethylammonium Groups. 2. Investigation of the Microphase Separation Transition

R. J. Goddard and S. L. Cooper*,†

Department of Chemical Engineering, University of Wisconsin–Madison, Madison, Wisconsin 53706

Received August 30, 1994; Revised Manuscript Received December 16, 1994®

ABSTRACT: The temperature dependence of the microstructure in a polyurethane cationomer, with an ion content of 0.47 mequiv/g, is investigated using small-angle X-ray scattering (SAXS) studies and dynamic viscoelastic measurements. Both techniques indicate considerable microphase mixing occurs in the melt, with the SAXS invariant and dynamic storage modulus decreasing abruptly near the onset of melt flow at approximately 85 °C. Although the trends are qualitatively similar to those observed at the microphase separation transition (MST) in conventional polyurethanes, the presence of a MST cannot be stated conclusively since some level of the heterogeneous lamellar morphology persists to the highest accessible experimental temperature of 150 °C.

Introduction

In the preceding paper,[1] results of FTIR temperature studies suggested that the specific interaction responsible for the substantial increase in mechanical properties of the title polyurethane (PU) cationomers is an interchain hydrogen bond between the urethane N–H group and the neutralizing anion of the trialkylammonium group. Further, we proposed that the viscous flow transition in dynamic mechanical thermal analysis was directly related to the observed shift in N–H bonding from the anion to urethane carbonyls at elevated temperatures. Our earlier investigation of these same PU cationomers showed that the unquaternized precursor polymer is essentially a homogeneous material.[2] This raises the obvious question: If hydrogen bonding between N–H groups and anions is the primary driving force for microphase separation, and the number of N–H to anion bonds diminishes at elevated temperatures, then do the PU cationomers pass through a microphase separation transition (MST) at temperatures near the onset of viscous flow?

The MST or order–disorder transition has been extensively studied in diblock and triblock copolymers. Various experimental techniques such as small-angle X-ray scattering (SAXS),[3–11] differential scanning calorimetry (DSC),[12,13] and melt rheology[14–21] have been used to distinguish between homogeneous and heterogeneous morphologies. In spite of their commercial importance, far fewer investigations of the MST have been reported for segmented polyurethane elastomers. Using a combination of SAXS and DSC, Koberstein and co-workers[22,23] concluded that the onset of microphase mixing in polyurethanes with hard segments of 4,4′-diphenylmethane diisocyanate (MDI) and butanediol (BD) was at temperatures below the melting point of the microcrystalline hard domains (T_m). Isothermal crystallization below the apparent MST temperature (T_{MST}) occurred within the confines of existing hard domains, since microphase separation preceded crystallization. At temperatures between T_{MST} and T_m, hard-segment crystallization took place from a homogeneous melt.[23] Koberstein and Galambos also investigated the origin of multiple melting endotherms in this material.[24] Simultaneous SAXS–DSC experiments and wide-angle X-ray diffraction profiles at various temperatures suggested that the endotherms were associated with distinct crystal populations of different melting points. Since the melting occurred at temperatures above T_{MST}, melted hard-segment material at each endotherm spontaneously mixed with the soft microphase. The onset of microphase mixing was indicated in SAXS results by a drastic decrease in the invariant over a temperature range of 30–40 °C, and a coincident sharp increase in the long period, with complete disappearance of the interference peak above T_m.[23,24] Almost identical observations were reported by Chu and co-workers in SAXS temperature studies of a similar polyurethane with MDI/BD hard segments.[25] In a separate study, they also used SAXS to measure the kinetics of structure development in segmented polyurethanes quenched from the homogeneous melt to temperatures below T_{MST}.[26] Ryan *et al.* examined the order–disorder transition in a multiblock polyurethane with amorphous hard domains.[27] Like the polyurethanes with semicrystalline hard segments, SAXS profiles of the amorphous PU showed a sharp decrease in the invariant as the temperature increased through the MST, with a corresponding abrupt change in the Bragg spacing. Also, rheological experiments showed that the low-frequency shear storage modulus decreased by roughly 1 order of magnitude as the temperature was increased through the MST, with less temperature dependence above and below the transition.

In the present work, the prospect of a MST in polyurethane cationomers was investigated using SAXS and rheological techniques. Since the experimental temperature range was limited by dequaternization, MST studies of a segmented PU with semicrystalline hard domains and a binary mixture of diblock copolymers were used for comparison.

Experimental Section

Two polyurethane cationomers, with ion contents of 0.47 and 0.88 mequiv/g and a nominal hard-segment content of 50%, were used in the present study. The soft segment for both polymers, the structures of which are shown in Figure 1, is

* To whom correspondence should be addressed.
† Present address: College of Engineering, University of Delaware, Newark, DE 19716.
® Abstract published in *Advance ACS Abstracts,* February 1, 1995.

0024-9297/95/2228-1401$09.00/0

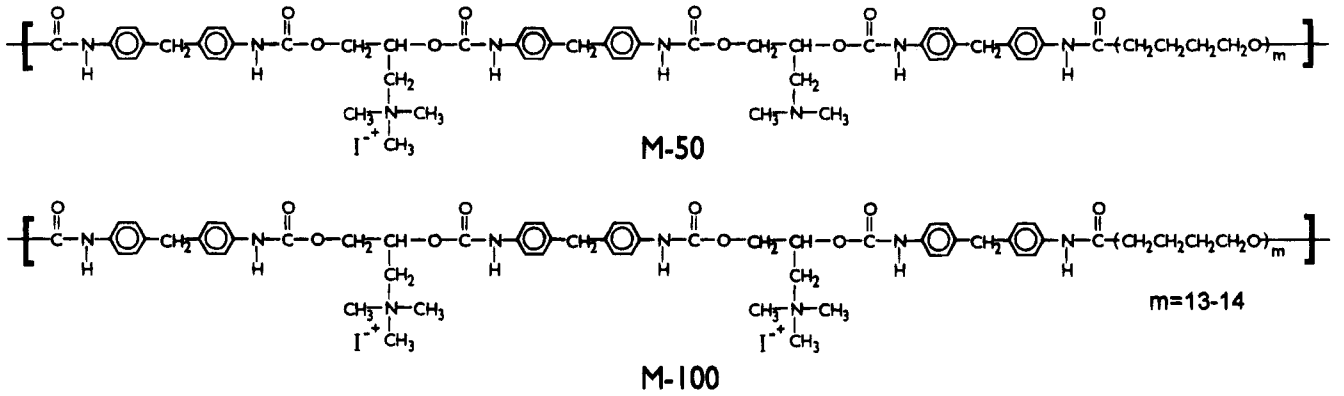

Figure 1. Chemical structures of the polyurethane cationomers.

Table 1. Extent of Dequaternization As Measured by Weight Loss and Iodine Content

temp[a] (°C)	% I^-	% wt loss	% dequaternization: I^- basis	% dequaternization: wt basis[b]
initial	11.87			
110	11.50	0.8	3	5
145	10.77	3.8	9	25
180	4.53	15.9	60	110

[a] 3 h in dry nitrogen. [b] Assumes Hoffmann-type elimination.

poly(tetramethylene oxide) (PTMO, $M_n = 990$). Hard segments of the two materials are comprised of MDI chain-extended with either 3-(trimethylammonio)-1,2-propanediol iodide (TMPI) or a mixture of TMPI and 3-(dimethylamino)-1,2-propanediol (DMP). The cationomers were prepared via a two-step polymerization in *N,N*-dimethylacetamide (DMAc) as described previously.[2] Samples are denoted M-###, where ### is the mole percent of TMPI as chain extender. To prepare samples for infrared spectroscopy, the cationomers were solution cast from anhydrous DMAc (Aldrich). Most of the solvent was evaporated with dry air at 50 °C; residual solvent was removed by placing the samples in a vacuum oven at 50–55 °C for 4 days and then at room temperature for 1–3 days. For X-ray scattering temperature studies and rheological measurements, the cationomer M-50 was compression molded into circular disks (25 mm diameter) at 130 °C and 60 MPa for 4 min.

Infrared Spectroscopy. Samples for infrared analysis were cast directly onto sodium chloride windows from a 1% (w/v) solution of the cationomer in DMAc. Film thicknesses were adjusted such that the maximum absorbance of any band was less than 0.7 to be conservatively within the absorbance range where the Beer–Lambert law is valid.[28] Spectra were acquired on a Mattson Model GL-5020 using a MCT detector at a resolution of 2 cm^{-1}; a minimum of 64 scans were averaged for each spectrum. Samples were heated to elevated temperatures in a dry nitrogen atmosphere by placing the polymer/NaCl sample in a well-insulated homemade temperature cell with resistance heaters and NaCl windows. The temperature was measured at the surface of the sample and was controlled to within 0.5 °C using a proportional–integral–derivative (PID) controller tuned to eliminate overshoot. All spectra were corrected for extraneous background absorbance and normalized for differences in sample thickness according to protocol described previously.[1]

Small-Angle X-ray Scattering (SAXS). Scattering profiles were collected using a Kratky camera with a Braun Model OED-50M linear position sensitive detector. Cu Kα X-rays (wavelength $\lambda = 1.54$ Å, $E = 8042$ eV) were generated by an Elliot GX-21 rotating anode, with $K\beta$ radiation attenuated by nickel foil. For optimal signal-to-noise, the sample thickness t was selected such that the product μt was approximately equal to one, where μ is the absorption coefficient at 8042 eV. The cationomer M-50 was molded into an annular brass ring of the appropriate thickness and covered on both sides with high-temperature Kapton tape to minimize thickness changes associated with viscous flow at elevated temperatures. SAXS patterns were obtained at elevated temperatures by heating the sample in a home-built heating cell, with the sample held at the target temperature for 30 min prior to data collection. Two resistance temperature detectors measured the temperature on either side of the polymer, and control of ±1 °C was provided by a PID controller tuned to eliminate overshoot. Both t and μt were determined before and after each SAXS profile to monitor possible sample flow and dequaternization at elevated temperatures.

Table 2. Dequaternization As Indicated by Changes in the N–H Stretching Vibration

temp[a] (°C)	M-100 ϵ	M-100 detectable[b] dequaternization	M-50 ϵ	M-50 detectable[b] dequaternization
130	0.997	no	0.998	no
140	0.998	no	0.999	no
150	0.984	marginal	0.999	no
160	0.983	marginal	0.999	no
170	0.868	yes	0.986	yes
180	0.776	yes	0.938	yes

[a] 20 min in dry nitrogen. [b] See text for criteria.

Scattering patterns were corrected for parasitic scattering, sample transmittance, the Kapton windows, and detector sensitivity and linearity along the wire. A dead time correction was not warranted since total count rates were less than 200 s^{-1}. Channel-to-angle calibration was determined with a cholesterol myristate sample, and all intensities were adjusted to an absolute basis using a previously calibrated Lupolen standard. SAXS patterns were desmeared according to the iterative procedure of Lake.[29] All data are reported as I/I_eV versus q, where I is the measured intensity, I_e is the scattered intensity from a single electron, and V is the scattering volume. The scattering vector q is equal to $4\pi \sin\theta/\lambda$, where 2θ is the scattering angle. In our previous SAXS studies of PU cationomers, a sample-to-detector distance of about 60 cm was used.[2] In the present study, the sample-to-detector distance was decreased to approximately 38 cm to obtain adequate counts in less time. Although the shorter distance also increased the experimental range of q, all profiles were truncated at $q = 2.5$ nm^{-1} for consistency with the earlier study. Subtraction of background scattering, determination of the one-dimensional Bragg spacing, and calculation of the invariant were as formerly detailed.[2]

Measurement of Dynamic Viscoelastic Properties. The dynamic storage modulus G' and loss modulus G'' were determined in a nitrogen atmosphere using a Bohlin VOR melt rheometer in the oscillatory shear mode at temperatures of 60–150 °C. Sample geometry was defined by 25-mm-diameter parallel plates at a gap of approximately 0.5 mm; the gap dimension was corrected for thermal expansion of the apparatus. Measurements were obtained as isothermal frequency scans, at increasing angular frequency ω from about 0.01 to 100 rad/s. Each isothermal scan was conducted at a fixed strain amplitude, well within the linear viscoelastic regime, with strains ranging from 0.05% at 60 °C to 9% at 150 °C.

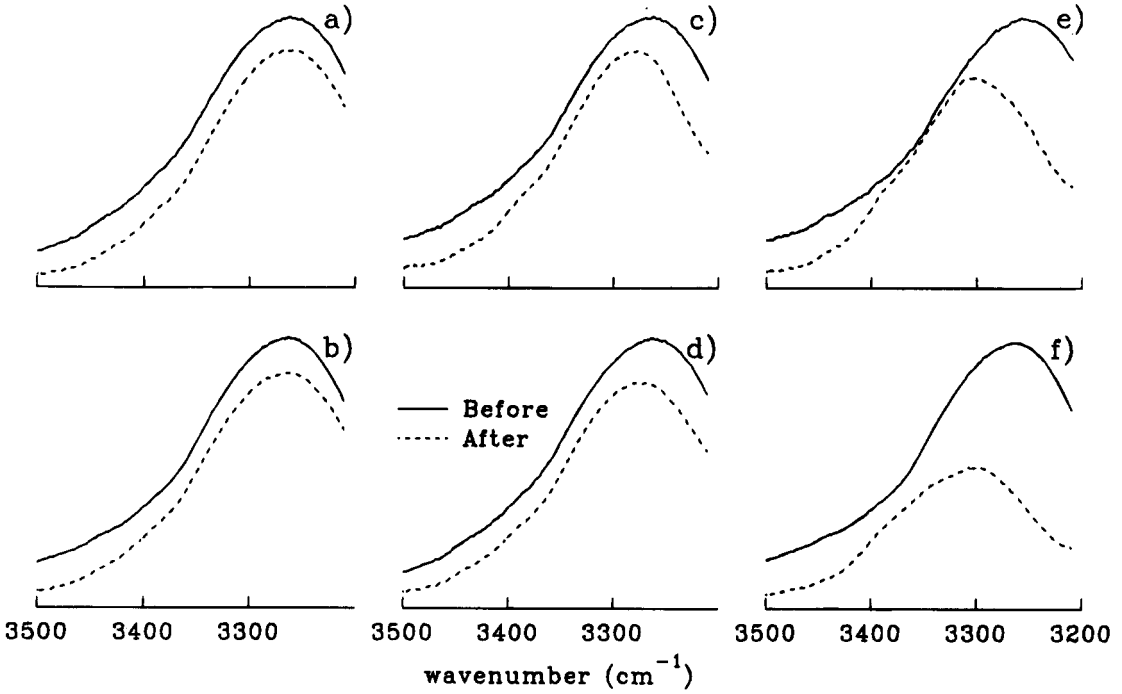

Figure 2. FTIR spectra of M-100 in the N–H stretching region before and after 20 min of heating at (a) 130, (b) 140, (c) 150, (d) 160, (e) 170, and (f) 180 °C.

Results and Discussion

Thermal studies of any polymer system can be jeopardized by decomposition, and the ammonium groups of cationomers are particularly susceptible. The extent of dequaternization is clearly a function of both time and temperature. However, as opposed to performing a full kinetic study, we chose to determine only the upper temperature at which dequaternization would not significantly affect results. For a rotating-anode X-ray source, data collection times of 2–4 h were anticipated at each temperature. The percent dequaternization that might occur during SAXS measurements was estimated by heating thin polymer films (0.2 mm) in a nitrogen atmosphere for 3 h. Results of the test for the cationomer M-100 are given in Table 1, where the percent dequaternization was defined according to weight loss and the elemental iodine content (Galbraith Laboratories). For calculations based on the percentage weight loss, a Hoffmann-type elimination was assumed in which hydriodic acid and trimethylamine are the elimination products. Charlier *et al.* found that this mechanism was the most likely mode of degradation in telechelic polystyrenes with quaternary ammonium end groups.[30] Two points can be readily inferred from the results of Table 1. First and most importantly, the upper temperature limit for SAXS experiments will be somewhere in the range of 110–140 °C. We have implicitly assumed that a few percent dequaternization will not significantly alter the cationomer morphology. Secondly, an additional mechanism(s) of degradation is evident since levels of dequaternization calculated from weight loss were always greater than levels determined from iodine content, and the Hoffmann-type elimination has the maximum theoretical weight loss of dequaternization. Results suggest the second type of degradation occurs at temperatures as low as 110 °C. Some mode of degradation catalyzed by the hydriodic acid eliminated during dequaternization is likely, since polyurethanes typically show much better thermal stability.

Although a few percent dequaternization is tolerable in SAXS studies, this is not true for rheological experiments where subtle transitions in viscoelastic properties are being investigated. If we want to define experimental conditions where essentially no dequaternization occurs, the weight loss and elemental analysis methods of quantifying dequaternization are not accurate enough. However, our previous investigation suggested that the N–H stretching region of infrared spectra was very sensitive to even small levels of dequaternization.[1] The following procedure was developed to determine the upper temperature limit for rheological experiments. The cationomers were heated in a nitrogen atmosphere from room temperature to some elevated temperature in 2–3 min, held at that temperature for 20 min, and then cooled back to room temperature in 5–7 min. FTIR spectra were recorded before and after heating and compared to determine if the process was reversible. In addition to looking for qualitative differences in the spectra, before and after spectra were compared mathematically. If we assume that the after spectrum can be "mapped" onto the before spectrum with an offset constant B and multiplication factor M according to eq 1,

$$A_{\text{after}}(\nu) = M \times A_{\text{before}}(\nu) + B \qquad (1)$$

then the linear least-squares fit of the absorbances A over all wavelengths ν yields a correlation coefficient ϵ that quantifies the similarity in shape of the spectra before and after heating. The constant B eliminates the effect of slight differences in baseline subtraction, while M adjusts for small errors in normalization for sample thickness.

Correlation coefficients for both cationomers at temperatures from 130 to 180 °C are given in Table 2, with the before and after spectra of the N–H stretching region displayed in Figure 2 for M-100 and Figure 3 for M-50. At least 12 samples of each cationomer were correlated to each other prior to heating. Sample-to-sample comparisons of M-100 all gave values of ϵ greater than 0.990, and greater than 0.995 for M-50. These

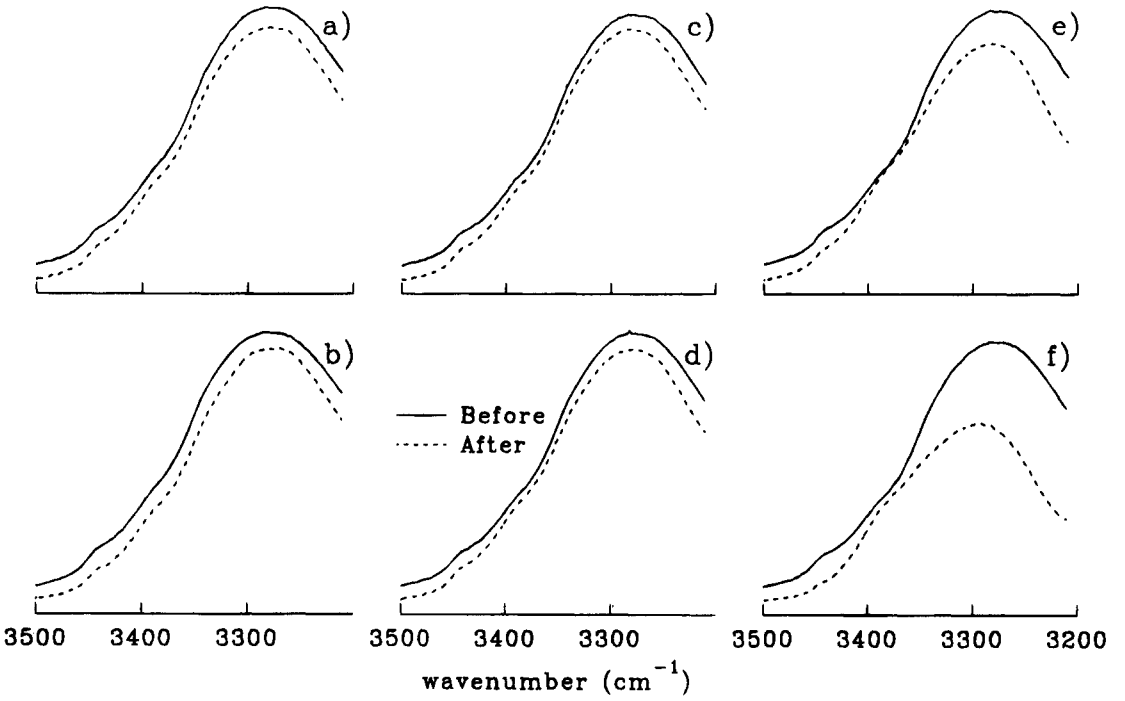

Figure 3. Same as Figure 2, except sample is M-50.

values were used as the criteria to determine if before and after spectra at a given temperature were "identical". Heating for 20 min at 170 °C and higher clearly resulted in irreversible changes to the N–H stretching region of both cationomers. At temperatures at or below 140 °C, the process for both cationomers appears fully reversible. The heating of sample M-100 to temperatures between 150 and 160 °C was only slightly irreversible as evidenced by a subtle convergence of before and after spectra around 3350 cm^{-1} and correlation coefficients just below 0.990. For sample M-50, values of ϵ would imply reversibility at 150 and 160 °C. However, the subtle convergence around 3350 cm^{-1} described for M-100 was also evident for sample M-50. Based on these results, a maximum temperature of 150 °C was selected for dynamic viscoelastic measurements.

Results of the brief dequaternization study also suggested that further investigation of the MST for the cationomer M-100 would be fruitless, since experiments in the temperature regime of viscous flow would be compromised by dequaternization. However, the upper transition in dynamic mechanical thermal analysis of sample M-50 is only around 85 °C.[2] A "temperature window" therefore exists, between the onset of viscous flow and the experimental temperature limits defined by dequaternization, where a homogeneous melt might be observed.

Figure 4 shows SAXS profiles of the cationomer M-50 at temperatures from 30 to 130 °C, after subtraction of background scattering. Data collection times ranged from 4 h at room temperature to 2 h at 110 and 130 °C. The SAXS curve at room temperature displayed a single interference maxima at $q = 0.65$ nm^{-1}. In our earlier investigation, this peak was attributed to a periodic arrangement of lamellar hard and soft domains analogous to that found in conventional polyurethane elastomers.[2] From 30 to 70 °C, the intensity of the peak increased approximately 10%, while the position of the peak was essentially unchanged. Above 70 °C there was a clear change in the scattering curves, as the intensity of the maxima decreased substantially and the peak position shifted to lower wave vectors with increasing temperature. The decrease in intensity was much

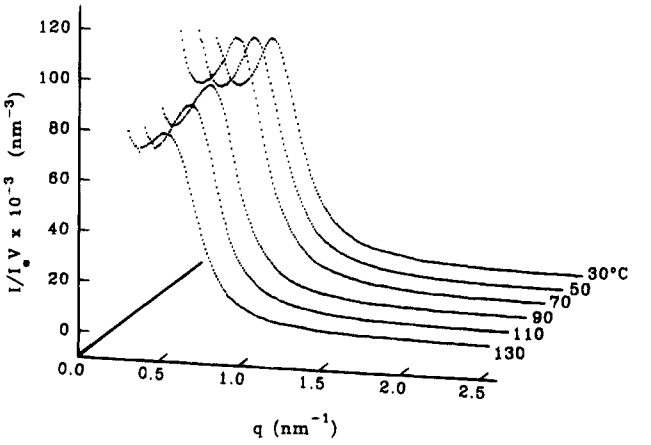

Figure 4. Temperature dependence of SAXS profiles for M-50.

greater than might be explained by dequaternization, because μ was constant (within experimental error of 5%) before and after SAXS data collection at all temperatures. This indicates that less than 7% dequaternization occurred, since iodine atoms absorb greater than 75% of the X-rays.

Differences in morphology as a function of temperature were quantified by first multiplying the scattered intensity by q^2. Bragg's law was applied to the peak of the corrected profile to evaluate the interlamellar spacing $L_{1\text{-D}}$, while the extent of microphase mixing is reflected in the total integrated scattered intensity, or invariant Q, given by eq 2.

$$\frac{Q}{V} = \int_0^\infty q^2 I(q)\, dq \qquad (2)$$

Morphological parameters are summarized in Table 3 and displayed graphically as a function of temperature in Figure 5. Also included in Figure 5 are data from Galambos for a segmented PU with semicrystalline hard domains of MDI/BD.[31] Three temperature regions are generally observed for conventional polyurethanes. At low temperatures, Q increases with temperature while the interdomain spacing may increase slightly or remain

Table 3. SAXS Parameters at Various Temperatures

temp (°C)	$L_{1\text{-}D}$ (nm)	Q/V (nm^{-6})
30	9.6	31 000
50	9.5	32 600
70	9.5	35 800
90	10.0	31 100
110	10.3	25 900
130	10.9	20 700

constant. Previous researchers have postulated a variety of phenomena that could explain the trends in this region including increased purity of the microphases[32] and thermal expansion.[25,27,32] Next, a temperature regime exists where the invariant decreases sharply with increasing temperature. Since the invariant is independent of the size and shape of the domains, the sharp decrease in Q results from increased microphase mixing and the consequent loss of electron density contrast as indicated by the equation[33]

$$\frac{Q}{V} = 2\pi^2\phi_1\phi_2(\varrho_1 - \varrho_2)^2 \qquad (3)$$

where ϕ_i and ϱ_i are the volume fraction and electron density, respectively, of each microphase. Above T_{MST} the invariant plateaus, and the interdomain spacing becomes ill-defined as the interference peak decays beyond distinction. Although the highest experimental temperature for M-50 was limited to 130 °C by dequaternization, the same general behavior was observed. Only the plateau region at high temperatures was absent. From 30 to 70 °C, the invariant increased 15%, while the interlamellar distance was unchanged. In the transition region between 90 and the maximum experimental temperature of 130 °C, the repeat distance increased approximately 15% and the invariant decreased over 40%. For the PU cationomers, these results indicate that considerable microphase mixing accompanies the onset of viscous flow and shift in N–H bonding from the anions to urethane carbonyls. However, some evidence of the lamellar structure still exists in the melt to temperatures of at least 130 °C.

The rheological properties of the cationomer M-50 are shown in Figure 6, where G' and G'' are plotted versus frequency at various temperatures from 60 to 150 °C. At temperatures up to approximately 100 °C, complex rheological behavior with a relatively weak ω-dependence was observed. At the lowest frequencies, both G' and G'' approached the lines proportional to $\omega^{1/2}$ that have been observed in previous investigations of ordered diblock and triblock copolymers.[17,21,34] The ω-dependence of G' and G'' increased with increasing temperature, although at 150 °C the storage modulus still had a slope less steep than the line $G' \sim \omega^2$ which is expected for homopolymers and homogeneous copolymers. At 150 °C, the loss modulus closely matches the anticipated result $G'' \sim \omega$ for homogeneous polymer melts. These results are consistent with those of SAXS and suggest that the rheological behavior of the cationomer approaches that of a homogeneous material, but some heterogeneity still exists at the highest experimental temperature.

In Figure 7, the same G' data are replotted as isochronal temperature curves. Symmetric monodisperse diblock and triblock copolymers frequently show a sharp discontinuity in G' at T_{MST} at low frequencies.[16,17,19] At increased frequencies, the transition broadens and shifts to higher temperatures. A discontinuous drop in G' was not observed for the PU cationomer at even the lowest test frequency of 0.063 rad/s

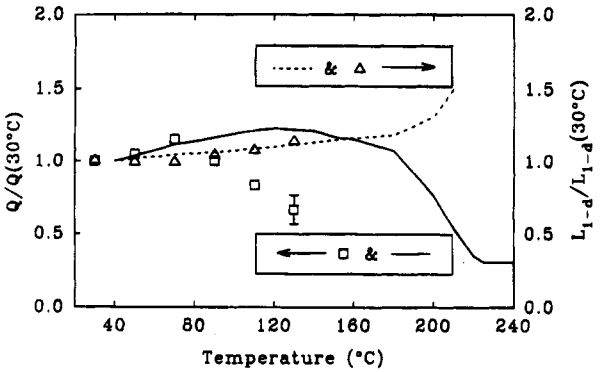

Figure 5. Small-angle X-ray scattering invariant and interlamellar repeat distance of the cationomer M-50 (symbols) from patterns of Figure 4. Also included are data from Galambos for a PU with MDI/BD hard segments (lines).[31] All data were normalized to the values at 30 °C.

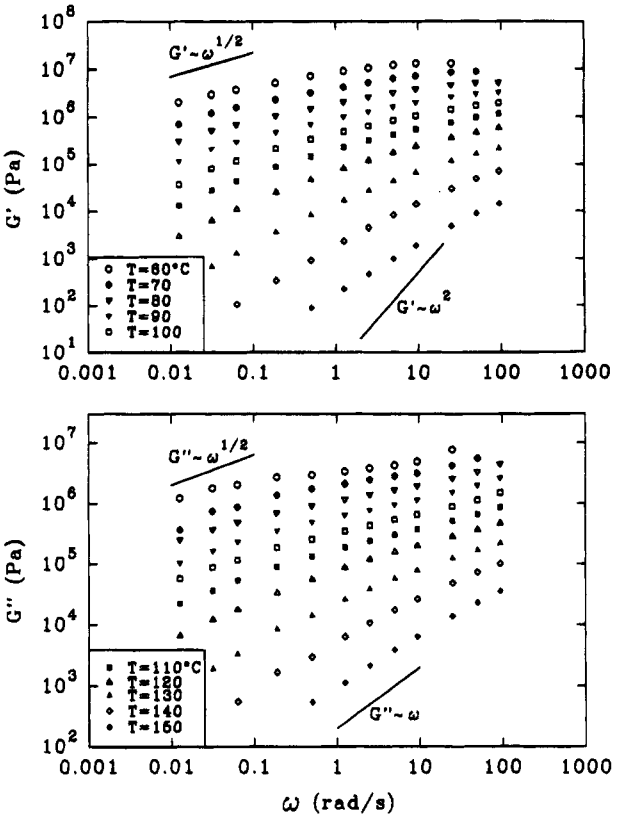

Figure 6. Dynamic storage modulus G' (top) and loss modulus G'' (bottom) of M-50 in the temperature interval 60–150 °C

However, a relatively sharp decline was observed starting around 110 °C. Similar results, shown by the dashed line of Figure 7, were reported by Almdal *et al.*[3] for a binary mixture of diblock copolymers of the same composition but different block lengths. Their results showed that even modest asymmetries and polydispersities of the blocks led to an order–disorder transition with continuous character. They speculated the broad transition was a biphasic region, where the fraction of the disordered phase increased with increasing temperature. Although the trends in Figure 7 are similar the cationomer does not show the high-temperature plateau corresponding to a homogeneous phase seen in the diblock copolymer mixture.

Isochronal curves at higher frequencies were shifted to higher temperatures as expected, but the ω-dependence was less than is often noted for diblock and triblock copolymers. Gouinlock and Porter reported that the greatest frequency dependence occurs around the

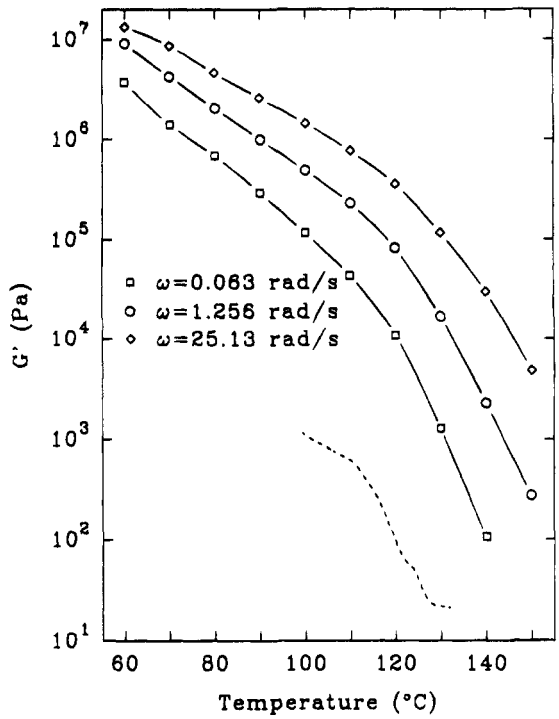

Figure 7. Isochronal plots of G' versus temperature for sample M-50 (solid lines). Included for comparison are data for a binary mixture of diblock copolymers of the same composition but different block lengths (dashed line).[35]

critical reduced frequency for the polymer, above which no domain disruption occurs.[16] The critical frequency is a strong function of molecular weight as well as the copolymer composition. For the present segmented PU cationomers, extraction of individual chain segments from a domain would likely have a relatively short relaxation time due to the smaller block lengths compared to diblock and triblock copolymers. A shorter relaxation time corresponds to a higher critical frequency, which for the sample M-50 is apparently above the greatest test frequency of 100 rad/s. A weak ω-dependence was also recently shown for a styrene–isoprene diblock copolymer with liquid-like order (i.e., the domains were not ordered onto a lattice) by Adams and co-workers.[36]

Conclusions

A broad flow transition, starting around 85 °C, was previously observed in PU cationomers with pendant trialkylammonium groups using dynamic mechanical thermal analysis; the specific interaction responsible for microphase separation in these materials was found to diminish in the same temperature regime. In the present investigation, both SAXS and rheological experiments indicate considerable microphase mixing occurs near the onset of viscous flow. The SAXS invariant begins decreasing between 70 and 90 °C and drops over 40% by 130 °C. An increase in the ω-dependence of G' and G'' starts around 110 °C, and at 150 °C the rheological behavior approaches that of a homogeneous copolymer or homopolymer. When replotted as a function of temperature, a sharp but continuous decrease in the low-frequency storage modulus is apparent beginning at 100 °C. Whether or not these changes are part of a broad MST is inconclusive. Although the trends of both techniques agree qualitatively with investigations of the MST in more conventional multiblock copolymers and less-ordered block copolymers, and extensive microphase mixing is clearly evident, a homogenous melt was not observed. Dequaternization limited the upper temperature of SAXS and rheological experiments to 130 and 150 °C, respectively, and a lamellar microstructure was still apparent in the melt at the highest temperatures.

Acknowledgment. Support for this work was provided by the U.S. Department of Energy under Grant DE-FG02-88ER45370 and the National Science Foundation through Grant DMR-90-16959. R.J.G. also gratefully acknowledges the support of the Department of Defense through the National Defense Science and Engineering Graduate Fellowship program.

References and Notes

(1) Goddard, R. J.; Cooper, S. L. *Macromolecules* **1995**, *28*, 1390.
(2) Goddard, R. J.; Cooper, S. L. *J. Polym. Sci., Part B: Polym. Phys.* **1994**, *32*, 1557.
(3) Widmaier, J. M.; Meyer, G. C. *J. Polym. Sci., Polym. Phys. Ed.* **1980**, *18*, 2217.
(4) Roe, R.-J.; Fishkis, M.; Chang, J. C. *Macromolecules* **1981**, *14*, 1091.
(5) Mori, K.; Hasegawa, H.; Hashimoto, T. *Polym. J.* **1985**, *17*, 799.
(6) Koberstein, J. T.; Russell, T. P.; Walsh, D. J.; Pottick, L. *Macromolecules* **1990**, *23*, 877.
(7) Sakurai, S.; Mori, K.; Okawara, A.; Kimishima, K.; Hashimoto, T. *Macromolecules* **1992**, *25*, 2679.
(8) Wolff, T.; Burger, C.; Ruland, W. *Macromolecules* **1993**, *26*, 1707.
(9) Hoffmann, A.; Koch, T.; Stühn, B. *Macromolecules* **1993**, *26*, 7288.
(10) Winter, H. H.; Scott, D. B.; Gronski, W.; Okamoto, S.; Hashimoto, T. *Macromolecules* **1993**, *26*, 7236.
(11) Winey, K. I.; Gobran, D. A.; Xu, Z.; Fetters, L. J.; Thomas, E. L. *Macromolecules* **1994**, *27*, 2392.
(12) Cohen, R. E.; Ramos, A. R. *Macromolecules* **1979**, *12*, 131.
(13) Bates, F. S.; Bair, H. E.; Hartney, M. A. *Macromolecules* **1984**, *17*, 1987.
(14) Kraus, G.; Naylor, F. E.; Rollmann, K. W. *J. Polym. Sci., Part A-2* **1971**, *9*, 1839.
(15) Chung, C. I.; Gale, C. G. *J. Polym. Sci., Polym. Phys. Ed.* **1976**, *14*, 1149.
(16) Gouinlock, E. V.; Porter, R. S. *Polym. Eng. Sci.* **1977**, *17*, 534.
(17) Bates, F. S. *Macromolecules* **1984**, *17*, 2607.
(18) Han, C. D.; Kim, J. *J. Polym. Sci., Part B: Polym. Phys.* **1987**, *25*, 1741.
(19) Han, C. D.; Baek, D. M.; Kim, J. K. *Macromolecules* **1990**, *23*, 561.
(20) Gehlsen, M. D.; Almdal, K.; Bates, F. S. *Macromolecules* **1992**, *25*, 939.
(21) Balsara, N. P.; Derahia, D.; Safinya, C. R.; Tirrell, M.; Lodge, T. P. *Macromolecules* **1992**, *25*, 3896.
(22) Leung, L. M.; Koberstein, J. T. *Macromolecules* **1986**, *19*, 706.
(23) Koberstein, J. T.; Russell, T. P. *Macromolecules* **1986**, *19*, 714.
(24) Koberstein, J. T.; Galambos, A. F. *Macromolecules* **1992**, *25*, 5618.
(25) Li, Y.; Gao, T.; Liu, J.; Linliu, K.; Desper, C. R.; Chu, B. *Macromolecules* **1992**, *25*, 7365.
(26) Chu, B.; Gao, T.; Li, Y.; Wang, J.; Desper, C. R.; Byrne, C. A. *Macromolecules* **1992**, *25*, 5724.
(27) Ryan, A. J.; Macosko, C. W.; Bras, W. *Macromolecules* **1992**, *25*, 6277.
(28) Koenig, J. L. *Spectroscopy of Polymers*; American Chemical Society: Washington, DC, 1992.
(29) Lake, J. A. *Acta Crystallogr.* **1967**, *23*, 191.
(30) Charlier, P.; Jérôme, R.; Teyssié, P.; Prud'homme, R. E. *J. Polym. Sci., Part A: Polym. Chem.* **1993**, *31*, 129.
(31) Galambos, A. F. Ph.D. Dissertation, Princeton University, 1989.
(32) Russell, T. P.; Jérôme, R.; Charlier, P.; Foucart, M. *Macromolecules* **1988**, *21*, 1709.
(33) Bonart, R.; Müller, E. H. *J. Macromol. Sci., Phys.* **1974**, *B10*, 177.
(34) Bates, F. S.; Rosedale, J. H.; Fredrickson, G. H. *J. Chem. Phys.* **1990**, *92*, 6255.
(35) Almdal, K.; Rosedale, J. H.; Bates, F. S. *Macromolecules* **1990**, *23*, 4336.
(36) Adams, J. L.; Graessley, W. W.; Register, R. A. *Polym. Prepr. (Am. Chem. Soc., Div. Polym. Chem.)* **1994**, *35* (1), 591.

MA941316S